MOLECULAR AND CELLULAR BIOLOGY, Mar. 1991, p. 1553–1565
0270-7306/91/031553-13$02.00/0

Vol. 11, No. 3

Activation of Tyrosine Kinase and Microfilament-Binding Functions of c-*abl* by *bcr* Sequences in *bcr/abl* Fusion Proteins

JOHN R. McWHIRTER AND JEAN Y. J. WANG*

Department of Biology and Center for Molecular Genetics, University of California San Diego, La Jolla, California 92093-0116

Received 22 August 1990/Accepted 12 December 1990

Chronic myelogenous leukemia and one type of acute lymphoblastic leukemia are characterized by a 9;22 chromosome translocation in which 5′ sequences of the *bcr* gene become fused to the c-*abl* proto-oncogene. The resulting chimeric genes encode *bcr/abl* fusion proteins which have deregulated tyrosine kinase activity and appear to play an important role in induction of these leukemias. A series of *bcr/abl* genes were constructed in which nested deletions of the *bcr* gene were fused to the c-*abl* gene. The fusion proteins encoded by these genes were assayed for autophosphorylation in vivo and for differences in subcellular localization. Our results demonstrate that *bcr* sequences activate two functions of c-*abl*: the tyrosine kinase activity and a previously undescribed microfilament-binding function. Two regions of *bcr* which activate these functions to different degrees have been mapped: amino acids 1 to 63 were strongly activating and amino acids 64 to 509 were weakly activating. The tyrosine kinase and microfilament-binding functions were not interdependent, as a kinase defective *bcr/abl* mutant still associated with actin filaments and a *bcr/abl* mutant lacking actin association still had deregulated kinase activity. Modification of actin filament functions by the *bcr/abl* tyrosine kinase may be an important event in leukemogenesis.

The c-*abl* proto-oncogene has been strongly implicated in the pathogenesis of Philadelphia chromosome (Ph′)-positive human leukemias. Chronic myelogenous leukemia (CML) and one type of acute lymphoblastic leukemia (ALL) are characterized by the clonal expansion of a hematopoietic stem cell containing a reciprocal translocation between chromosomes 9 and 22 (6, 11, 30). This Ph′ translocation results in the head-to-tail fusion of 5′ exons of the breakpoint cluster region (*bcr*) gene on chromosome 22 with the c-*abl* gene on chromosome 9 (21–24). These hybrid genes are transcribed into chimeric *bcr*/c-*abl* mRNAs in which exon 1 of c-*abl* is replaced by 5′ *bcr* exons (24, 39, 46, 47). *bcr*/c-*abl* fusion proteins are produced which contain the N-terminal 927 or 426 amino acids of *bcr* in CML and Ph′-positive ALL, respectively (1a, 8).

The oncogenic potential of these *bcr*/c-*abl* fusion proteins has been demonstrated in a variety of cell culture systems. Expression of the CML-specific $p210^{bcr/abl}$ protein in primary bone marrow cultures leads to transformation of pre-B lymphoid cells (37, 54). $P210^{bcr/abl}$ also transforms an interleukin-3-dependent lymphoblastoid cell line and partially transforms Rat-1 fibroblasts (9, 35). The $p185^{bcr/abl}$ protein associated with Ph′-positive ALL appears to have a higher transforming potency in vitro than $p210^{bcr/abl}$ (34, 38). Recently, in vivo mouse models for CML and Ph′-positive ALL have been developed which provide direct evidence for a role of *bcr/abl* proteins in these diseases (10, 20).

The c-*abl* proto-oncogene encodes a cytoplasmic protein tyrosine kinase (16, 41, 47, 53). Based on homology to other cytoplasmic tyrosine kinases, the c-*abl* protein can be divided into four domains: an N-terminal variable domain encoded by two alternative first exons, a kinase regulatory domain (SH3/SH2) with homology to the N-terminal noncatalytic domain of $p60^{c\text{-}src}$, a tyrosine kinase domain, and a large noncatalytic C-terminal domain with no sequence similarity to other tyrosine kinases. Like other cytoplasmic protein tyrosine kinases, the c-*abl* protein has an autokinase activity that is detectable in immune complex kinase assays (28). Autophosphorylation is also observed in vivo when c-*abl* is expressed in nonmammalian systems such as bacteria or insect cells (50). However, the autokinase activity of the c-*abl* protein is strongly inhibited in mammalian cells, suggesting that it is normally regulated by *trans*-acting factors (17). In contrast, the *bcr*/c-*abl* fusion proteins associated with Ph′-positive leukemias have deregulated autokinase activity in vivo (27). We have shown previously that in vivo inhibition of the c-*abl* kinase requires the presence of an N-terminal regulatory region encoded by c-*abl* exons 2 and 3 which includes the *src* homology 3 (SH3) domain (17, 25). The SH3 domain of c-*abl* is deleted in the v-*abl* oncogene of Abelson murine leukemia virus (A-MuLV), resulting in constitutive activation of the v-*abl* kinase (51). Interestingly, the SH3 domain of c-*abl* is intact in *bcr*/c-*abl* fusion proteins. This suggests that activation of the c-*abl* kinase in Ph′-positive leukemias occurs by a different mechanism.

We have studied this mechanism by expressing a set of *bcr*/c-*abl* fusion proteins containing nested deletions of *bcr* in CML cells and NIH 3T3 cells. The tyrosine phosphorylation levels and subcellular localizations of the proteins were examined. Our results show that fusion of the first 63 amino acids of *bcr* to c-*abl* strongly activates the c-*abl* kinase and increases its association with the actin cytoskeleton. Fusion of *bcr* amino acids 64 to 509 to c-*abl* weakly activates the c-*abl* kinase and causes a smaller increase in actin association.

MATERIALS AND METHODS

Cell culture. K562 cells (33) were maintained in RPMI 1640 medium with 10% inactivated fetal calf serum. NIH 3T3 and COS cells were maintained in Dulbecco modified Eagle medium with 10% calf serum. All cell lines were grown in a 5% CO_2 incubator at 37°C.

* Corresponding author.

Plasmid construction. Construction of the c-*ablPst* and c-*ablHinc* deletions has been described previously (17, 50). To make the *bcr*/c-*ablPst* constructs, the c-*abl* cDNA was cleaved partially with *Pst*I, end blunted with Klenow fragment, and fitted with a 6-bp *Xba*I linker. The *bcr* cDNA was cleaved at the indicated restriction sites within the *bcr* coding region, end blunted with Klenow fragment where necessary, and fitted with *Xba*I linkers of 6, 8, or 10 bp. Both cDNAs were then cleaved at the *Pvu*I site within the Amp^r gene of their pBR322 sequences. The *Pvu*I-*Xba*I fragment of the *bcr* cDNA containing the 5′ end of the *bcr* gene was ligated in frame to the *Xba*I-*Pvu*I c-*abl* fragment containing the c-*ablPst* coding region. The addition of *Xba*I linkers resulted in the addition of 2 or 3 amino acids at the *bcr*/*abl* junction (Leu-Glu or Ala-Leu-Glu). To make the S39-Nh509 and B64-Nh509 constructs, the Nh509 construct was cleaved partially with *Stu*I or *Bal*I, respectively, and the deleted N-terminal codons were replaced by a polylinker containing codons for Met-Ala-Ala-Ala-Lys for translation initiation. To make the Nh509/Nar construct, the Nh509 construct was cleaved partially with *Nar*I, blunted with Klenow fragment, and fitted with *Bam*HI linkers and the *Bam*HI fragment containing the Nh509/Nar gene was ligated into the pLJ and pSVL vectors.

To make the *lacZ*/c-*ablPst* construct, the c-*abl* cDNA was partially cleaved with *Pst*I, end blunted with Klenow fragment, and fitted with *Eco*RI linkers. The vector pCH110 (Pharmacia) was partially cleaved with *Eco*RI at the site within the *lacZ* coding region. Both plasmids were then cleaved with *Bam*HI. The *Eco*RI-*Bam*HI fragment of c-*abl* containing the c-*ablPst* coding region was ligated into the *Eco*RI-*Bam*HI fragment of pCH110 so that the *lacZ* coding region was in frame with that of c-*ablPst*.

Construction of the lg/v-*abl* and sg/c-*ablPst* genes has been described previously (17). To make the lg/c-*ablPst* construct, the *Hinc*II-*Bam*HI fragment of lg/v-*abl* containing the v-*abl* sequences was removed and replaced by the *Xba*I-*Bam*HI fragment of Nh509 containing the c-*ablPst* sequences after fitting the *Hinc*II and blunted *Xba*I ends with *Bam*HI linkers.

All constructs were inserted into the cloning sites of the retroviral expression vector pLJ or the simian virus 40 expression vector pSVL (17, 50). The maintenance of open reading frames in the fusion genes was confirmed by expressing the fusion proteins in COS cells and assaying their ability to be immunoprecipitated with antibodies for *abl* protein, *bcr* protein, β-galactosidase, or p15^{gag}.

Cell transfections. NIH 3T3 cells were cotransfected with 1 μg of pLJ construct and 10 μg of the replication-competent Moloney murine leukemia virus clone pZAP by using a modified calcium phosphate coprecipitation method as previously described (17). Two days after transfection, cells were split 1:4 and selected for resistance to G418. Cells were harvested 8 to 14 days later. K562 cells were transfected with pLJ constructs by electroporation with a BTX Transfector 300 (BTX, Inc., San Diego, Calif.). Cells were washed and resuspended to 10^7/ml in *N*-2-hydroxyethylpiperazine-*N*′-2-ethanesulfonic acid (HEPES)-buffered saline containing 10 μg of plasmid plus 90 μg of salmon sperm DNA per ml. They were pulsed at 500 V/cm and 1,100 μF. At 10 min after the pulse, the cells were diluted into serum-containing medium. Two days later, cells were cloned by limiting dilution in medium containing G418. G418-resistant clones were obtained at a frequency of approximately 1 in 10^4 cells. COS cells were transfected in 6-cm dishes with 4 μg of pSVL construct by the DEAE-dextran method as previously described (50).

Antibodies. Monoclonal antibody 8E9 and polyclonal anti-phosphotyrosine and anti-*abl* antibodies were made as previously described (43, 49). Anti-t/*bcr* antiserum was made against a small t-antigen/*bcr* fusion protein produced in bacteria. The t/*bcr* fusion gene was constructed by inserting the 1.3-kb *Xmn*I-*Bam*HI restriction fragment of *bcr* into the *Bgl*II cloning site of the vector pCS4 (52). The resulting gene contains the N-terminal 80 codons of simian virus 40 t antigen fused to codons 176 to 633 of *bcr*. Anti-*bcr* 1-16 antiserum was the gift of Ralph B. Arlinghaus and was made against a synthetic peptide corresponding to the N-terminal 16 amino acids of *bcr* (1).

Immunoprecipitations and immunoblotting. K562 or NIH 3T3 cells were lysed at approximately 2.5×10^6 cells per ml in IP lysis buffer (10 mM Tris-HCl [pH 7.5], 130 mM NaCl, 5 mM EDTA, 1% Triton X-100, 1 mg of bovine serum albumin [BSA] per ml, 20 mM sodium phosphate [pH 7.5], 10 mM sodium PP_i [pH 7.0], 50 mM NaF, 1 mM sodium orthovanadate, 1 mM phenylmethylsulfonyl fluoride, 1× protease inhibitor cocktail [10 μM benzamidine-HCl, 10 μg each of phenanthroline, aprotonin, leupeptin, and pepstatin per ml]). Lysates were precleared by ultracentrifugation at 100,000 × *g* for 30 min at 4°C and incubated overnight with either polyclonal anti-*abl* antiserum (49) or anti-*bcr* 1-16 antiserum. Immune complexes were precipitated by the standard method with formaldehyde-fixed *Staphylococcus aureus* (49). After being washed, the immune complexes were boiled in 2% sodium dodecyl sulfate (SDS) sample buffer and separated on SDS-polyacrylamide gels. Immunoblotting was done as previously described (49).

Detergent extraction assay. Cells were extracted as described by Boss et al. (4) with some modifications. K562 cells grown in suspension were washed once with cold phosphate-buffered saline (PBS) and once with CSK buffer [10 mM piperazine-*N*,*N*′-bis(2-ethanesulfonic acid) (PIPES; pH 6.8), 100 mM KCl, 300 mM sucrose, 2.5 mM $MgCl_2$]). They were then extracted twice for 2 min each at 3×10^7 cells per ml and 4°C with CSK extraction buffer (CSK buffer plus 0.5% Triton X-100, 1 mM sodium orthovanadate, 1 mM phenylmethylsulfonyl fluoride, and 1× protease inhibitor cocktail). Each extraction was followed by centrifugation at 1,000 × *g* for 5 min. The two supernatants were combined to make up the soluble (SOL) fraction. The pellet or detergent-insoluble matrix (DIM) fraction was resuspended to 10^7 cell equivalents per ml in CSK extraction buffer. As a total cell lysate control, an equal number of cells were washed and suspended to 10^7/ml in CSK extraction buffer. The fractions were boiled in 2% SDS sample buffer. Protein concentrations were determined by the Lowry assay. Extraction of NIH 3T3 cells was carried out on monolayer cells grown in 10-cm dishes. The same procedure was followed, except that the volume of CSK extraction buffer used for the SOL and DIM fractions was 0.7 and 0.35 ml per 10-cm dish, respectively.

Immunofluorescence. NIH 3T3 cells stably transfected with pLJ constructs and COS cells transiently transfected with pSVL constructs were seeded onto glass coverslips at a density of 1×10^4/cm^2. The next day they were washed twice with PBS. For anti-*abl* immunofluorescence, cells were fixed and permeabilized for 10 min at −20°C with methanol-acetone (7:3), dried for 15 min in a laminar flow hood, rehydrated in cold PBS, and washed with solution A (PBS, 0.1% BSA, 0.05% sodium azide). For double-label immunofluorescence with anti-*abl* plus phalloidin, cells were

fixed for 5 min with 3% formaldehyde in PBS, permeabilized for 5 min with 0.5% Triton X-100, and washed with solution A. All cells were stained for 30 min with either monoclonal anti-*abl* 8E9 antiserum (10 μg/ml) or polyclonal t-*bcr* antiserum (1:800), washed with solution A, stained for 30 min with rhodamine-conjugated goat anti-mouse antibody (Cappel), and then washed again with solution A. For staining of NIH 3T3 cells, cells were prestained for 15 min with 2% normal goat serum, and all subsequent antibody solutions contained 2% normal goat serum. For double staining of actin filaments, fluorescein-conjugated phalloidin was added to the secondary antibody solution. The cells were mounted with 0.2% *p*-phenylenediamine as an antiquenching agent, and epifluorescence microscopy was performed by using a Nikon fluorescence microscope. Kodak Tri-X 400 black-and-white 35-mm film was used to photograph cells.

RESULTS

Expression of *bcr*/c-*abl* fusion proteins. In the chimeric *bcr/abl* mRNAs characteristic of Ph′ chromosome-positive human leukemias, the 5′ variable exon of c-*abl* is deleted and replaced by *bcr* sequences (Fig. 1B, $p210^{bcr/abl}$). To determine which of these two alterations causes the c-*abl* tyrosine kinase to become deregulated, we constructed a mutant, c-*ablPst*, in which the 5′ variable exon plus four codons of the common region of the mouse c-*abl* cDNA have been replaced by a start codon followed by an alanine codon (Fig. 1B) (50). We have shown previously that the c-*ablPst* protein does not contain detectable phosphotyrosine when expressed in NIH 3T3 cells (17). This was also the case when the protein was expressed in the CML cell line K562 (data not shown). Thus, deletion of the variable domain of c-*abl* is not sufficient to activate its autokinase.

To study the effects of *bcr* sequences on the c-*abl* kinase, a set of nested deletions of a human *bcr* cDNA were ligated in frame to the 5′ end of the c-*ablPst* gene to create hybrid cDNAs which encode a series of *bcr*/c-*ablPst* fusion proteins (Fig. 1B). To determine whether viral *gag* sequences could contribute to deregulation of the c-*abl* kinase and to compare their effects with those of *bcr* sequences, we made two constructs, sg(small *gag*)/c-*ablPst* and lg(large *gag*)/c-*ablPst*, which encode *gag*/c-*ablPst* fusion proteins containing the N-terminal 35 or 235 amino acids of the Moloney murine leukemia virus *gag* gene, respectively (Fig. 1C). To control for nonspecific effects on the c-*abl* kinase due to fusion of an arbitrary polypeptide to the c-*ablPst* protein, we constructed a hybrid gene, *lacZ*/c-*ablPst*, which encodes a β-galactosidase/c-*ablPst* fusion protein (Fig. 1C). As positive controls we used two deregulated forms of the c-*abl* tyrosine kinase: *gag*/v-*abl* (referred to here as lg/v-*abl*) and c-*ablHinc*, a gene in which the 5′ variable exon plus 93 codons of the common region have been replaced by a start codon followed by an alanine codon (Fig. 1C) (17). This deletion is very similar to the one found in lg/v-*abl* and has been shown to deregulate the c-*abl* kinase (17).

To express these proteins, the constructs were inserted into the *Bam*HI cloning site of the retroviral expression vector pLJ (29), which also expresses the neomycin resistance (Neo^r) gene. The c-*ablPst*, *bcr*/c-*ablPst*, and control genes are expressed from the Moloney murine leukemia virus long terminal repeat, and the Neo^r gene is expressed from the internal simian virus 40 early promoter of pLJ. The CML cell line K562 (33) and NIH 3T3 fibroblasts were transfected with the pLJ constructs as described in Materials and Methods. Stably transfected cells were selected with G418 and screened for expression of *abl* proteins by immunoblotting cell lysates with a monoclonal antibody for the *abl* protein (49).

Fusion of *bcr* sequences to the c-*ablPst* protein deregulates its autokinase activity. To measure the phosphotyrosine (PTyr) content of an *abl* protein, G418-resistant populations of NIH 3T3 cells expressing that protein were lysed and the *abl* proteins were first immunoprecipitated with a polyclonal antibody for the *abl* protein and then immunoblotted with either an antibody for PTyr (Fig. 2B) or a monoclonal antibody for the *abl* protein (Fig. 2A). To allow detection of low levels of autokinase activity, some cells were treated with 50 μM sodium orthovanadate, an inhibitor of protein tyrosine phosphatases, for 7 h prior to cell lysis (Fig. 2, + lanes). The PTyr-to-*abl* protein ratio determined from these immunoblots is a relative measure of the stoichiometry of autophosphorylation. Representative results of NIH 3T3 expression are shown in Fig. 2. The PTyr-to-*abl* protein ratios of proteins expressed in NIH 3T3 cells are listed in Table 1.

The longest *bcr/abl* fusion protein constructed for this study was Nh509, in which the N-terminal 509 codons of *bcr* are fused to the c-*ablPst* gene (Fig. 1B). The Nh509 protein was found to contain a high level of PTyr, and its PTyr-to-*abl* protein ratio was comparable to that of $p210^{bcr/abl}$ (Fig. 2, lanes 11 and 12; Table 1). The PTyr-to-*abl* protein ratio of Nh509 protein was 12-fold greater than that of c-*ablHinc* and 6-fold greater than that of lg/v-*abl* (Table 1). These differences were consistently observed in several experiments. These results show that fusion of *bcr* sequences to c-*abl* activates the c-*abl* autokinase more efficiently than does deletion of the SH3 domain.

To ensure that this activating effect is due specifically to the *bcr* sequences, we examined two *gag*/c-*ablPst* fusion proteins, lg/c-*ablPst* and sg/c-*ablPst*, and a β-galactosidase/c-*ablPst* fusion protein, *lacZ*/c-*ablPst* (Fig. 1C). We have previously shown that addition of a 35-amino-acid fragment of *gag* protein to the c-*ablPst* protein does not activate the c-*abl* tyrosine kinase and that the A-MuLV transforming protein, $p160^{lg/v\text{-}abl}$, is activated primarily by deletion of the SH3 domain of c-*abl* (17). Consistent with previous results, no effect on autokinase activity was observed when only the N-terminal 35 amino acids of *gag* were fused to c-*ablPst* (Table 1, sg/c-*ablPst*). However, the lg/c-*ablPst* fusion protein was found to contain extremely low levels of PTyr, only 0.5% of the level detected in Nh509 (Fig. 2, lane 5; Table 1). There was a 4- to 10-fold increase in this level after vanadate treatment (Fig. 2, lane 6; Table 1). This indicates that a low level of activation may be induced by the 235-amino-acid *gag* sequence. Fusion of the N-terminal 1,046 amino acids of β-galactosidase to the c-*ablPst* protein had no detectable effect on its PTyr level (Fig. 2, lanes 9 and 10; Table 1, *lacZ*/c-*ablPst*). These results show that the high stoichiometry of autophosphorylation of *bcr*/c-*ablPst* proteins is due to some unique property of *bcr*.

To demonstrate that the PTyr on Nh509 protein was due to autophosphorylation, we made an Nh509 construct by using a kinase-defective mutant of c-*abl*. This protein, NH509/His, is identical to Nh509 except for a Lys-to-His point mutation in the c-*abl* ATP-binding site (47a). No PTyr was detectable on the Nh509/His protein, indicating that tyrosine phosphorylation of Nh509 was dependent on c-*abl* kinase activity (Fig. 2, lane 17; Table 1). However, treatment with vanadate did lead to the accumulation of a very low level of PTyr on the Nh509/His protein (Fig. 2, lane 18; Table 1). It thus appears that the majority of the PTyr detected on Nh509 is

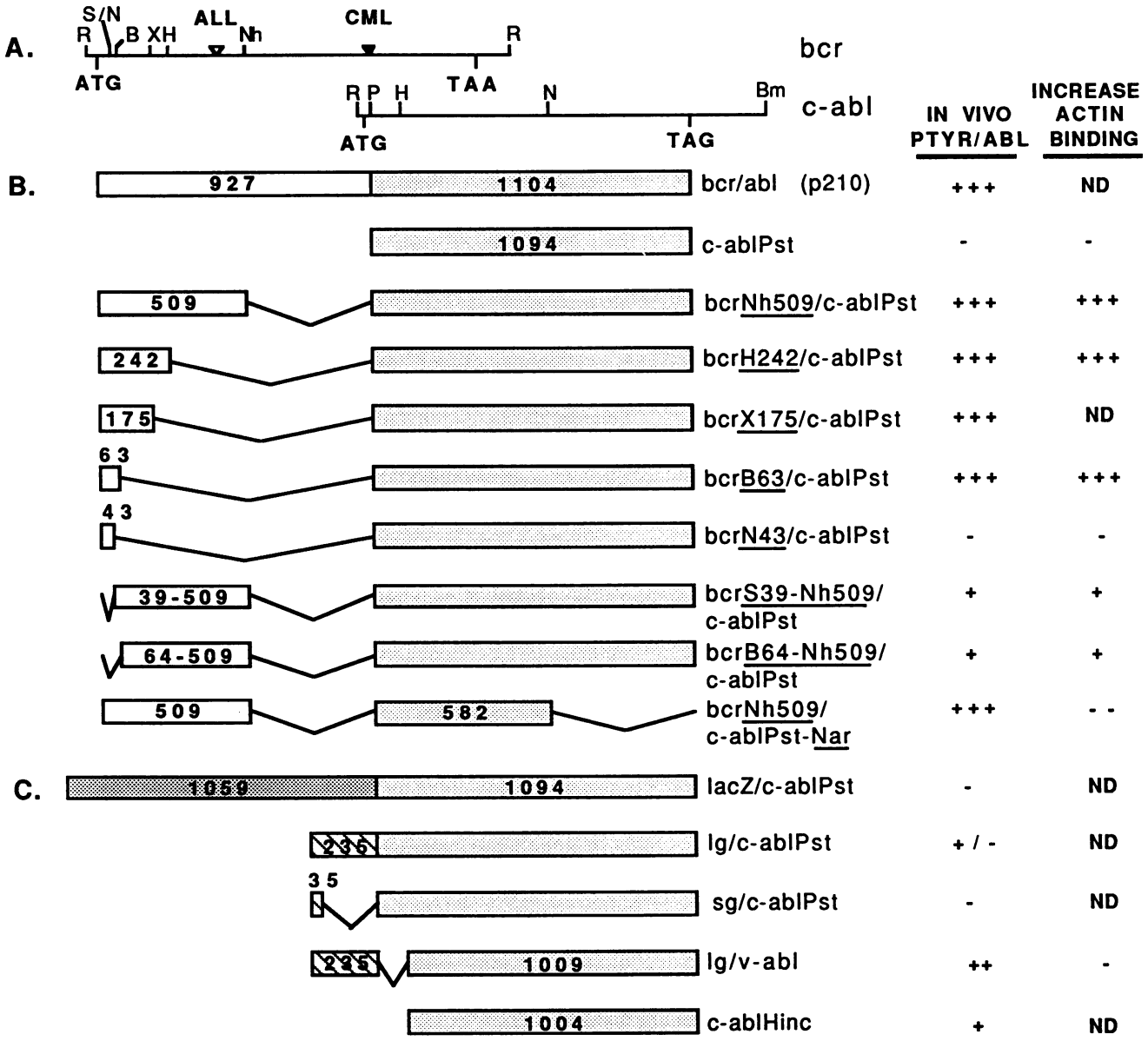

FIG. 1. Structures of c-*abl* fusion proteins. (A) Schematic representations of the human *bcr* and mouse c-*abl* cDNAs used to construct mutants. Horizontal lines represent DNA sequences. Restriction enzyme sites used to make deletions and fusions are indicated: R, *Eco*RI; S, *Stu*I; N, *Nar*I; B, *Bal*I; X, *Xmn*I; H, *Hin*cII; Nh, *Nhe*I; P, *Pst*I; Bm, *Bam*HI. Locations of translational start (ATG) and stop (TAA, TAG) codons are shown. White and black arrowheads above *bcr* cDNA indicate the junctions where 5′ *bcr* sequences become fused in frame to the common exon sequences of c-*abl* in ALL and CML, respectively, to produce chimeric *bcr/abl* mRNAs. The ALL- and CML-specific *bcr/abl* mRNAs contain 426 and 927 *bcr* codons, respectively. (B) Structures of the 5′ variable exon-deleted c-*abl* mutant, c-*ablPst*, and the *bcr*/c-*ablPst* fusion constructs. Boxes represent protein-coding sequences. The *bcr* and c-*abl* sequences are aligned beneath their corresponding cDNAs in panel A. Symbols: ▭, *bcr* sequences; ▩, c-*abl* sequences. Numbers within boxes indicate the number of codons. *bcr/abl* (p210) is the transforming gene expressed by the CML cell line K562. c-*ablPst* is a 5′ variable exon-deleted mouse c-*abl* gene made by truncating the c-*abl* cDNA to the first *Pst*I site. The *bcr*/c-*ablPst* constructs contain the indicated codons of the human *bcr* cDNA fused in frame to the mouse c-*ablPst* gene. For brevity, these *bcr*/c-*ablPst* fusion genes will be referred to in the text by letters indicating the restriction enzyme sites used to truncate the *bcr* cDNA followed by numbers indicating the number of *bcr* codons fused to c-*ablPst* (underlined portions of names). The last 512 c-*abl* codons of Nh509 were deleted to make the Nh509/*Nar* gene. (C) Structures of c-*abl* mutants used as controls. Symbols: ▩, c-*abl* sequences; ▥, *lacZ* sequences; ▨, A-MuLV-derived *gag* sequences. *lacZ*/c-*ablPst* encodes a β-galactosidase/c-*ablPst* fusion protein containing the N-terminal 1,059 amino acids of β-galactosidase. lg/c-*ablPst* and sg/c-*ablPst* are fusions of the entire 235-codon *gag* region (lg, large *gag*) or only the first 35 codons (sg, small *gag*) of the A-MuLV transforming gene lg/v-*abl* to c-*ablPst*. c-*ablHinc* is a 5′-truncated c-*abl* gene that is missing the entire 5′ variable exon plus 93 codons of the common region. This deletion is approximately the same as the one in lg/v-*abl*. The column headed "in vivo Ptyr/*abl*" contains a summary of the relative stoichiometries of in vivo autophosphorylation of *abl* proteins as determined by immunoblotting with antibodies for PTyr and *abl*, based on results shown in Fig. 2 and Table 1. The column headed "increased actin binding" contains a summary of results from indirect immunofluorescence experiments shown in Fig. 4 and 5. ND, Not determined.

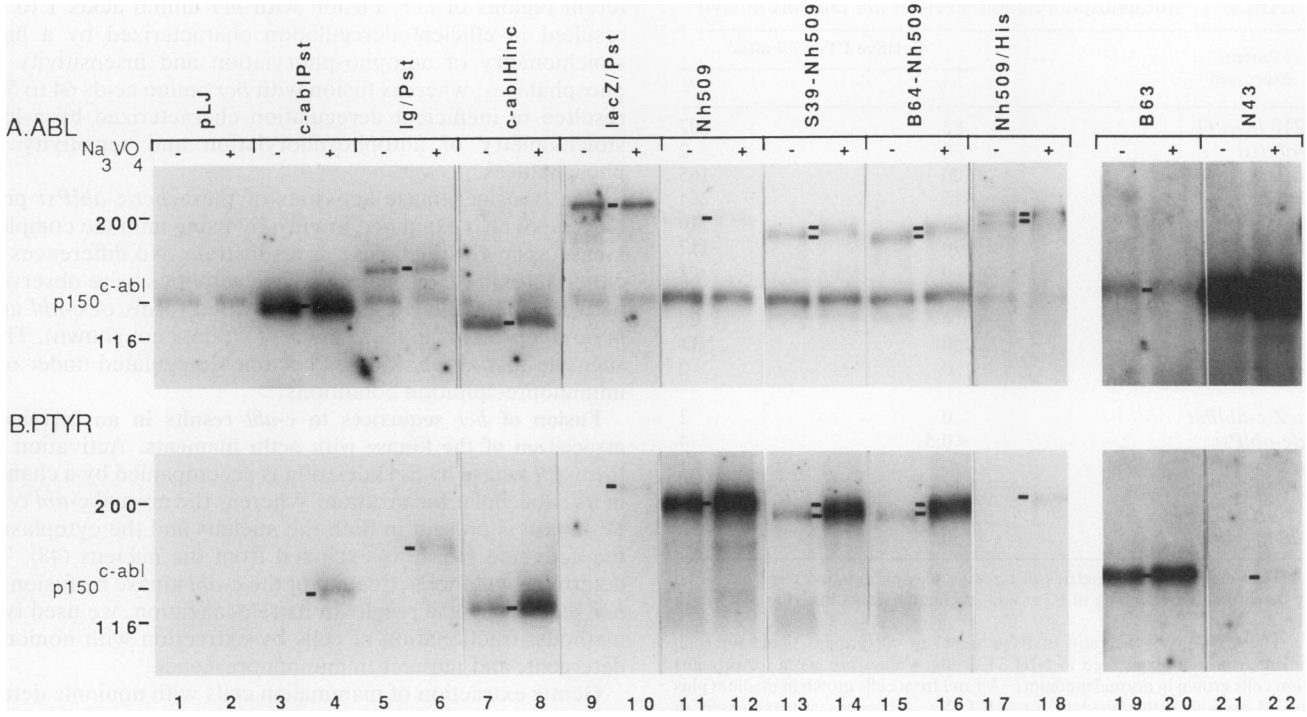

FIG. 2. Mapping of the kinase-activating regions of *bcr*. NIH 3T3 fibroblasts were cotransfected with pZAP and the indicated pLJ constructs. Following G418 selection, polyclonal populations of cells were treated with normal medium (− lanes) or with medium containing 50 μM Na_3VO_4 (+ lanes) for 7 h. They were then lysed in IP lysis buffer and immunoprecipitated with a polyclonal antibody for *abl* protein. Because the fusion proteins B63 and N43 (lanes 19 to 22) comigrate with the endogenous $p150^{c\text{-}abl}$ protein on SDS gels, they were immunoprecipitated with anti-*bcr* 1-16 antiserum rather than with the antibody for *abl* protein. The immunoprecipitates were boiled in 2% SDS buffer, separated on SDS–6.5% polyacrylamide gels, transferred to nitrocellulose, and immunoblotted either with monoclonal anti-*abl* antibody 8E9 (A) or with an affinity-purified antibody for PTyr (B). The positions of molecular weight markers and $p150^{c\text{-}abl}$ are shown on the left. (A) *abl* immunoblot; (B) Ptyr immunoblot. Proteins in lanes 1 to 18 were detected by autoradiography for approximately 2 weeks at room temperature, whereas those in lanes 19 to 22 were detected by autoradiography for 24 h at −80°C with an intensifying screen.

due to autophosphorylation, although some of the PTyr may be due to phosphorylation by another tyrosine kinase.

Two regions of *bcr* cause different degrees of c-*abl* kinase activation. Having determined that *bcr* sequences were required for activation of the c-*abl* autokinase in *bcr*/c-*abl* fusion proteins, we proceeded to map the minimal region of *bcr* which can carry out this function. A set of nested deletions in the *bcr* portion of the Nh509 fusion gene was made (Fig. 1B). Four of these constructs, H242, X175, B63, and N43, encode *bcr*/c-*ablPst* fusion proteins containing the N-terminal 242, 175, 63, and 43 amino acids of *bcr*, respectively (Fig. 1B). Two of them, S39-Nh509 and B64-Nh509, contain 5′ deletions so that the resulting fusion proteins are missing the N-terminal 38 and 63 amino acids of Nh509, respectively (Fig. 1B). The deleted N-terminal codons were replaced with a start codon followed by three alanine codons to express the proteins.

These *bcr*/c-*ablPst* genes were expressed in NIH 3T3 cells. Some of the proteins, including Nh509, appeared to be toxic to the cells as indicated by reduced transfection efficiencies, slower growth and instability of G418-resistant clones expressing the proteins, and a lower average level of protein expression. This toxic effect was correlated with the presence of the N-terminal 63 amino acids of *bcr* in the fusion protein (Fig. 2A, compare the *bcr*/*abl* protein level in lanes 19 and 20 with that in lanes 21 and 22).

The levels of autophosphorylation of these proteins in NIH 3T3 cells were compared with that of Nh509 (Fig. 2; Table 1). Because the fusion proteins B63 and N43 comigrate on SDS-polyacrylamide gel electrophoresis (PAGE) with the endogenous c-*abl* protein, they were immunoprecipitated with antibodies for the *bcr* protein before being immunoblotted with antibodies for PTyr and *abl* protein (Fig. 2, lanes 19 to 22). Comparison of the PTyr-to-*abl* ratios of the deleted *bcr*/c-*ablPst* proteins revealed that the N-terminal 63 amino acids of *bcr* are sufficient to deregulate the c-*ablPst* autokinase (Fig. 2, lanes 19 and 20; Table 1, compare H242, X175, and B63 with Nh509). Further truncation of the *bcr* region to 43 N-terminal amino acids completely abolished the ability of *bcr* to deregulate the c-*ablPst* autokinase: no PTyr was detected on N43 except for a low level seen after vanadate treatment (Fig. 2, lanes 21 and 22; Table 1). Deletion of the N-terminal 38 amino acids of Nh509, as in S39-Nh509, resulted in a 15-fold decrease in the PTyr level (Fig. 2, lane 13; Table 1). When the entire N-terminal 63-amino-acid region was deleted, as in B64-Nh509, a 25-fold decrease in PTyr level was observed (Fig. 2, lane 15; Table 1). This suggests that the N-terminal 63-amino-acid region is not only sufficient but also necessary to cause the majority of the autophosphorylation of Nh509. Although vanadate treatment caused only a 1.5- to 2-fold increase in the PTyr levels of most activated *abl* proteins (Table 1, c-*ablHinc*, Nh509, and B63), it caused a dramatic 4- to 8-fold increase in the PTyr levels of S39-Nh509 and B64-Nh509 (Fig. 3, lanes 14 and 16; Table 1). These results suggest that the c-*abl* autokinase can be deregulated independently by two dif-

TABLE 1. Autophosphorylation levels of *abl* proteins in vivo[a]

Protein expressed	Relative PTyr/*abl* ratio[b]	
	−V	+V
p210 *bcr/abl*	82	107
c-*ablPst*	0	2
Nh509	100	165
H242	115	264
X175	54	110
B63	70	117
N43	0	<1
S39-Nh509	6	33
B64-Nh509	4	24
Nh509/Nar	180	ND[c]
Nh509/His	0	2
lacZ/c-*ablPst*	0	2
lg/c-*ablPst*	<0.5	4
sg/c-*ablPst*	0	<1
lg/v-*abl*	16	50
c-*ablHin*c	8	15
c-*abl*	0	0

[a] The relative stoichiometries of tyrosine phosphorylation were measured by densitometric scanning of PTyr and *abl* immunoblots like those shown in Fig. 2.

[b] The table gives the ratio of PTyr signal to *abl* protein signal for each indicated protein expressed in NIH 3T3 cells. Values are given for proteins from cells grown in normal medium (−V) and from cells grown in medium plus 50 μM sodium orthovanadate for 7 h (+V). All values are expressed as percentages of the PTyr-to-*abl* protein ratio for Nh509 without vanadate treatment, which was set at 100 for each experiment.

[c] ND, Not determined.

ferent regions of *bcr*. Fusion with *bcr* amino acids 1 to 63 resulted in efficient deregulation characterized by a high stoichiometry of autophosphorylation and insensitivity to phosphatases, whereas fusion with *bcr* amino acids 64 to 509 resulted in inefficient deregulation characterized by a low stoichiometry of autophosphorylation and sensitivity to phosphatases.

The tyrosine kinase activities of these *bcr*/c-*ablPst* proteins were also examined in vitro by using immune complex kinase assays with enolase as a substrate. No differences in either autokinase or enolase kinase activities were observed between the activated and nonactivated forms of c-*abl* and *bcr*/c-*abl* proteins in these assays (17; data not shown). This suggests that all *abl* kinases become deregulated under our immunoprecipitation conditions.

Fusion of *bcr* sequences to c-*abl* results in an increased association of the kinase with actin filaments. Activation of the c-*abl* kinase by SH3 deletion is accompanied by a change in its subcellular localization. Whereas the normal c-*abl* type IV kinase is present in both the nucleus and the cytoplasm, the activated kinase is excluded from the nucleus (48). To determine whether activation of the c-*abl* kinase by fusion to *bcr* sequences also results in its relocalization, we used two methods: fractionation of cells by extraction with nonionic detergent, and indirect immunofluorescence.

Gentle extraction of mammalian cells with nonionic detergents removes the lipids and soluble proteins, leaving behind a DIM composed primarily of the nucleus, the cytoskeletal framework, and cytoskeleton-associated proteins (2, 5).

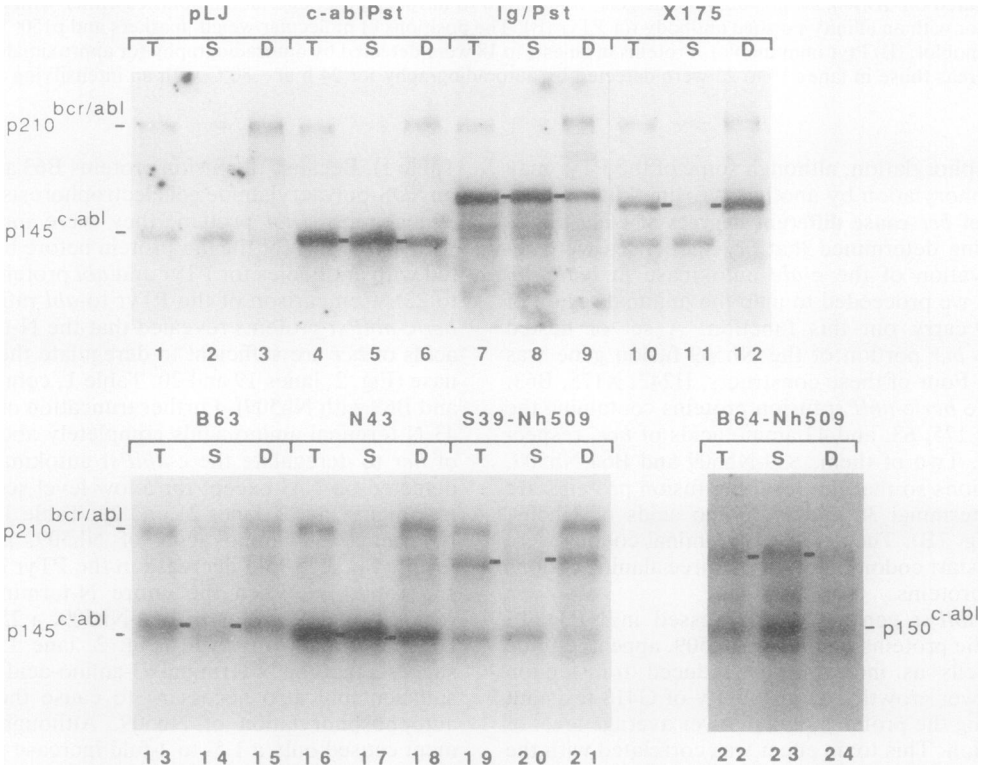

FIG. 3. Mapping of the *bcr* region responsible for increased association of *bcr/abl* proteins with the detergent-insoluble matrix. K562 cells (lanes 1 to 21) or NIH 3T3 cells (lanes 22 to 24) expressing the indicated *abl* proteins were extracted with CSK buffer containing 0.5% Triton X-100, and the fractions were boiled in 2% SDS sample buffer. Equal amounts of protein from each fraction were separated on SDS–6.5% polyacrylamide gels and immunoblotted with monoclonal anti-*abl* antibody 8E9. T, Total cell lysate; S, detergent-soluble fraction; D, DIM fraction. Positions of the endogenous $p145^{c\text{-}abl}$ and $p210^{bcr/abl}$ of K562 cells and the endogenous $p150^{c\text{-}abl}$ of NIH 3T3 cells are indicated.

TABLE 2. Distributions of *abl* proteins in soluble and insoluble fractions of cells extracted with Triton X-100[a]

Cell line	Protein expressed	% of TOT recovered[b]	Distribution[c]	
			%SOL	%DIM
K562	p210 *bcr/abl*	97	31	69
	c-*ablPst*	94	77	23
	Nh509	76	34	66
	H242	70	17	83
	X175	87	31	69
	B63	71	37	63
	N43	85	66	34
	S39-Nh509	72	51	49
	lg/c-*ablPst*	64	83	17
	sg/c-*ablPst*	91	71	29
	lg/v-*abl*	73	77	23
	c-*ablHinc*	97	70	30
	c-*abl*	97	79	21
NIH 3T3	Nh509	76	42	58
	B64-Nh509	82	84	16
	lg/v-*abl*	91	78	22
	c-*abl*	116	86	14
	p160 *bcr*	116	88	12

[a] K562 or NIH 3T3 cells expressing the indicated *abl* proteins or p160^{bcr} were detergent extracted and equal amounts of total protein from each fraction were immunoblotted with anti-*abl* antibody 8E9 or t/*bcr* antibody as described in Materials and Methods. The amount of *abl* (or *bcr*) protein per microgram of protein in each fraction was quantitated by densitometric scanning of the autoradiograms. It was determined by the Lowry assay that 36% of the total protein was recovered in the DIM fraction of K562 cells (or 30% for 3T3 cells). To determine the percentage of *abl* in the DIM or SOL fractions, the amount of *abl* protein per microgram of protein was multiplied by 0.36 and 0.64, respectively. This converted the values from units of *abl* per microgram of protein to *abl* per cell equivalent.

[b] This indicates the amount of *abl* protein recovered after detergent extraction as a percentage of the amount present in the total cell lysate (TOT) control. This is an indication of the amount of *abl* protein lost as a result of proteolytic degradation during the extraction procedure.

[c] To make it easier to compare between proteins, distributions are expressed as percentages of the *abl* protein recovered after extraction rather than as percentages of the total *abl* protein present before extraction.

Both p120$^{gag/v\text{-}abl}$ and p210$^{bcr/abl}$ have been reported to be associated with the DIM of transformed cell lines (4, 40). However, in these studies no comparisons were made with the distribution of normal c-*abl* protein. Therefore, this DIM association is of unknown significance.

We compared the distribution of p210$^{bcr/abl}$ with that of several other *abl* proteins after extraction of cell lines with a buffered salt solution containing 0.5% Triton X-100. Equal amounts of protein from each fraction were immunoblotted with a monoclonal antibody for *abl* protein. From these immunoblots the percentage of the total *abl* protein in each fraction was determined. These results are summarized in Table 2, and examples are shown in Fig. 3. On average, 69% of the p210$^{bcr/abl}$ was associated with the DIM in K562 cells (Fig. 3, all lanes; Table 2). In contrast, only 23% of the c-*ablPst* protein was recovered in this fraction (Fig. 3, lanes 4 to 6; Table 2). The sg/c-*ablPst*, c-*ablHinc*, and endogenous c-*abl* proteins had distributions similar to that of the c-*ablPst* protein (Fig. 3, lanes 1 to 3, p145$^{c\text{-}abl}$; Table 2). The *gag* fusion proteins lg/c-*ablPst* and lg/v-*abl* were consistently depleted in both fractions because 25 to 35% of these proteins were lost during the extraction, possibly as a result of proteolysis as indicated by the detection of lower-molecular-weight *abl* protein bands (Fig. 3, lanes 7 to 9; Table 2). Nevertheless, we estimate that no more than 23% of the lg/c-*ablPst* and lg/v-*abl* proteins are DIM associated. Similar results were obtained for *abl* proteins expressed in NIH 3T3 cells (Table 2, Nh509, lg/v-*abl*, and c-*abl*; data not shown). These results show that the *bcr/abl* fusion proteins p210$^{bcr/abl}$ and Nh509 have a much greater resistance to detergent extraction than do other *abl* proteins.

The subcellular localization of *bcr*/c-*ablPst* proteins was also examined by indirect immunofluorescence. Detection of *abl* proteins by this method requires that they be overexpressed. *abl* proteins have been shown to have similar subcellular localizations when they are overexpressed in COS cells to those when they are overexpressed in NIH 3T3 cells (38b, 48). Therefore, the *bcr*/c-*ablPst* genes were inserted into the COS cell expression vector pSVL and transfected into COS cells (50). After 2 days, indirect immunofluorescence was performed by using a monoclonal antibody for *abl* protein (Fig. 4).

Cells transfected with the pSVL vector alone had only faint, nonspecific background fluorescence (data not shown). The wild-type c-*abl*(IV) and c-*ablPst* proteins were localized throughout the nucleus and the cytoplasm (Fig. 4A). In most cells, the fluorescent intensity was slightly higher in the nucleus than in the cytoplasm. Within the nucleus, staining was excluded from the nucleoli. In some cells, we observed faint staining of cytoplasmic filaments which have been reported previously to colocalize with actin stress fibers (48). The Nh509 protein was localized exclusively in the cytoplasm and was highly concentrated in a complex meshwork of filaments (Fig. 4B). Most of these filaments appeared to run parallel to and immediately underneath the plasma membrane. Double-labeling experiments in which fluorescein isothiocyanate-conjugated phalloidin was used to stain F-actin revealed that Nh509 colocalizes with actin filaments. In COS cells, colocalization of Nh509 with both stress fibers and the meshwork or gel form of actin was observed (data not shown). An NIH 3T3 cell line that overproduces the Nh509 protein was also examined by double labeling. Consistent with results in COS cells, the Nh509 protein in NIH 3T3 cells was exclusively cytoplasmic and colocalized with stress fibers (Fig. 5B and C). Normal NIH 3T3 cells stained either with the *abl* antibody or purified rabbit immunoglobulin G had a diffuse, nonspecific background fluorescence (Fig. 5A).

Mapping of *bcr* sequences required for the increased actin association of *bcr/abl* proteins. The regions of *bcr* responsible for increased actin association of *bcr/abl* proteins were mapped both by detergent extraction and by indirect immunofluorescence of cells expressing nested deletions of *bcr*/c-*ablPst* (Fig. 1B; Table 2).

Detergent extraction was performed either on K562 clones or on polyclonal populations of NIH 3T3 cells expressing *bcr*/c-*ablPst* proteins (Fig. 3; Table 2). All fusion proteins containing the first 63 amino acids of *bcr* behaved like Nh509 in that they were 60 to 80% DIM associated (Fig. 3, lanes 10 to 15; Table 2, H242, X175, and B63). In contrast, the B64-Nh509 fusion protein behaved like c-*ablPst* in that it was only 16% DIM associated (Fig. 3, lanes 22 to 24; Table 2). Fusion proteins containing only part of the 63-amino-acid region had levels of DIM association intermediate between those of Nh509 and c-*ablPst*: the N43 fusion protein was 34% DIM associated and the S39-Nh509 fusion protein was 50% DIM associated (Fig. 3, lanes 16 to 21; Table 2). These results demonstrate that the region of *bcr* responsible for increased DIM association of *bcr/abl* proteins lies within the N-terminal 63 amino acids.

Association of the *bcr*/c-*ablPst* proteins with microfilaments was examined by indirect immunofluorescence of

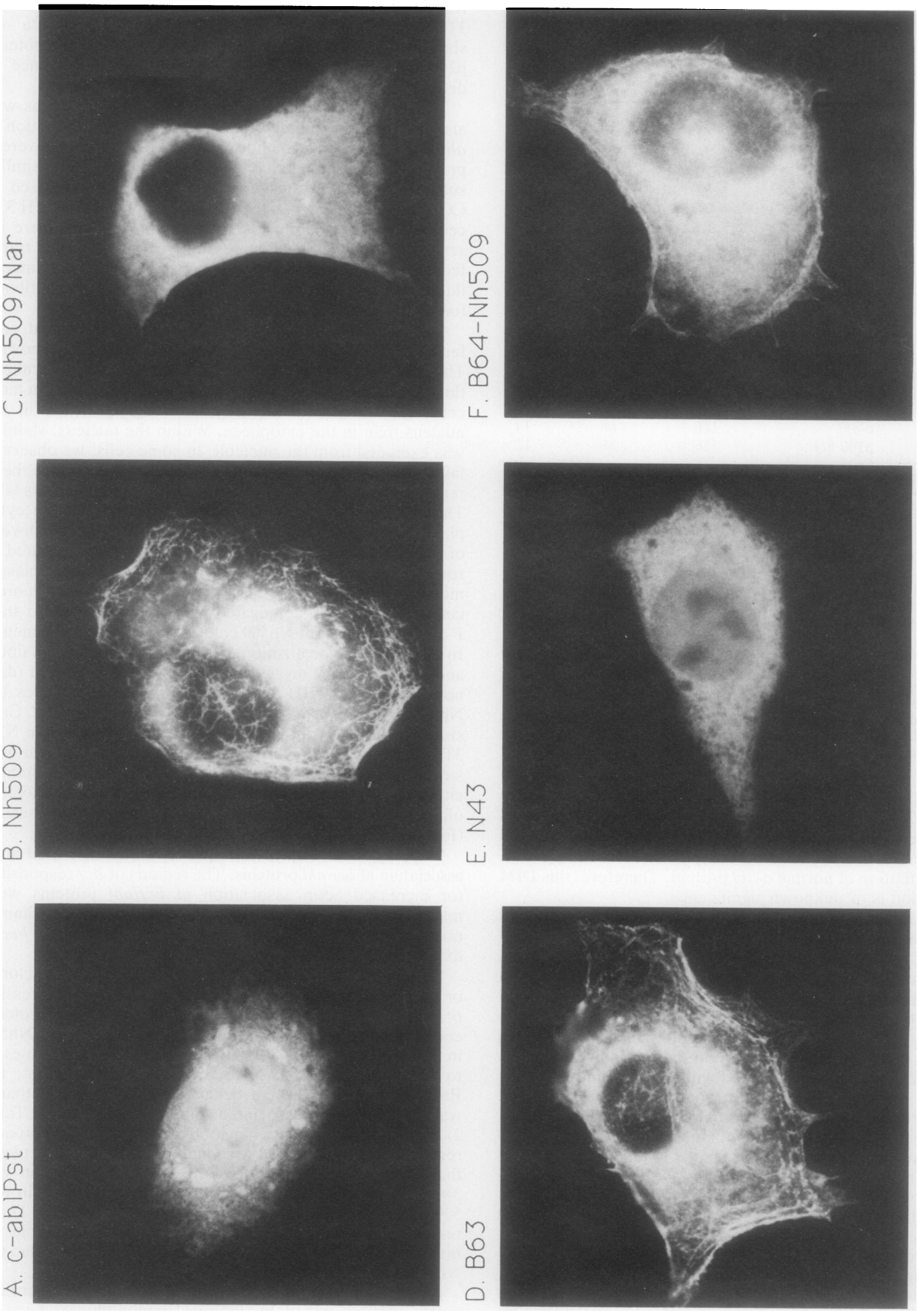

FIG. 4. Mapping of the *bcr* sequences necessary for increased actin filament association of *bcr/c-ablPst* fusion proteins by indirect immunofluorescence. At 2 days after transfection with the indicated pSVL constructs, COS cells were fixed and permeabilized with methanol-acetone and then stained for indirect immunofluorescence. The primary antibody was monoclonal anti-*abl* 8E9. The secondary antibody was rhodamine-conjugated goat anti-mouse antibody.

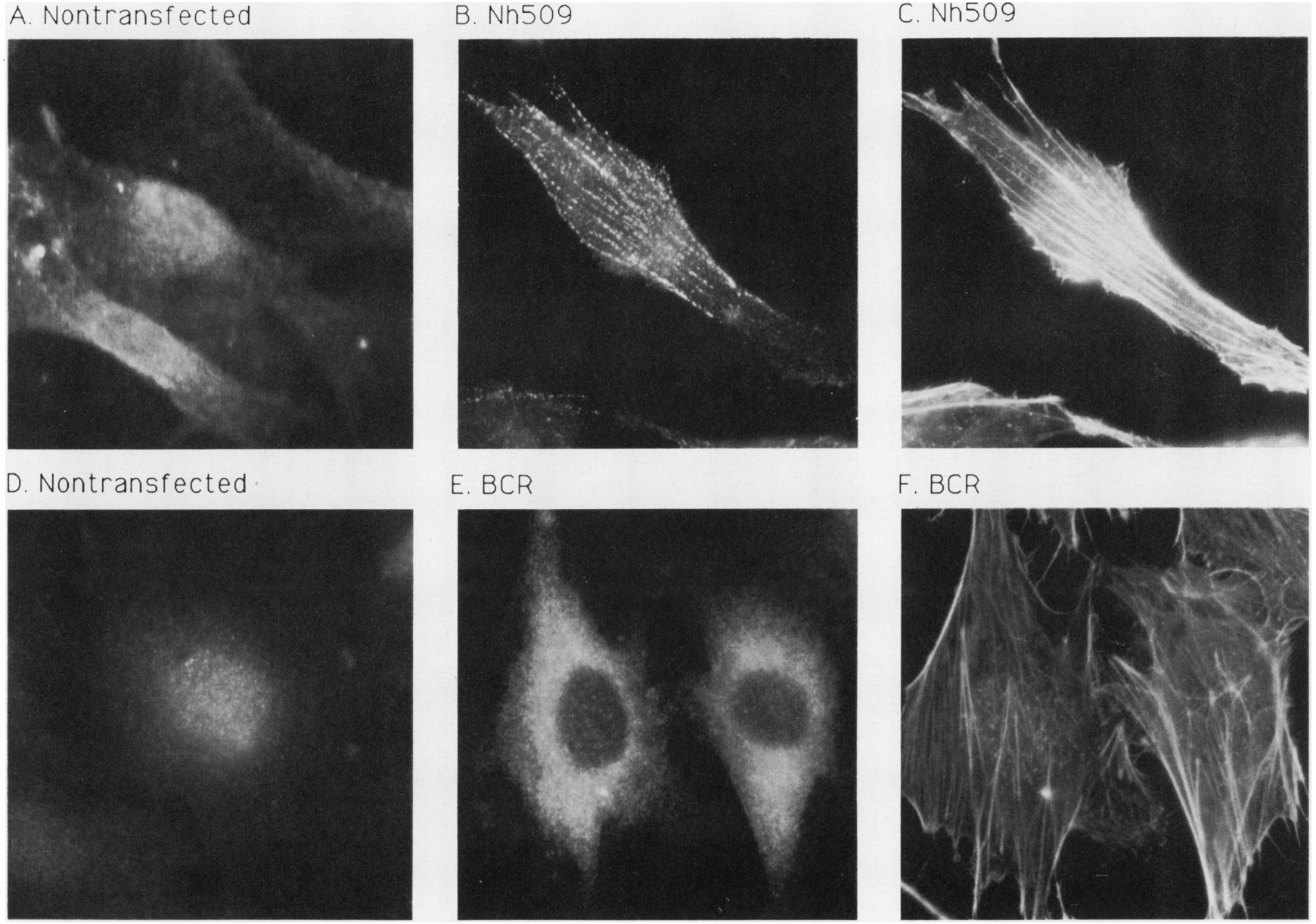

FIG. 5. Colocalization of the *bcr*/c-*ablPst* protein Nh509 with actin filaments demonstrated by double-label indirect immunofluorescence. NIH 3T3 cell lines were fixed with 3% formaldehyde in PBS, permeabilized with 0.5% Triton X-100, and stained for indirect immunofluorescence. Primary antibody was monoclonal anti-*abl* 8E9 antiserum (A to C) or polyclonal t/*bcr* antiserum (D to F). Secondary antibody was rhodamine-conjugated goat anti-mouse antibody (A to C) or rhodamine-conjugated goat anti-rabbit antibody (D to F), which was mixed with fluorescein isothiocyanate-conjugated phalloidin. (A and D) Nontransfected NIH 3T3 cells. Rhodamine signal showing nonspecific background staining. (B and C) NIH 3T3 cells overexpressing the *bcr*/c-*ablPst* protein Nh509. (D and E) NIH 3T3 cells overexpressing $p160^{bcr}$. (B and E) Rhodamine signal showing localization of Nh509 or or *bcr* proteins. (C and F) Fluorescein signal showing localization of F-actin in cells shown in panels B and E.

COS cells after transient transfection (Fig. 4; summarized in Fig. 1). All proteins containing *bcr* amino acids 1 to 63 behaved like Nh509 in that they were excluded from the nucleus and were associated predominantly with actin filaments (Fig. 4D). There appeared to be a slight reduction in the level of actin association of B63 relative to Nh509. In contrast, the N43 protein was localized diffusely throughout the nucleus and cytoplasm (Fig. 4E). This suggests that the N-terminal 43 amino acids of *bcr* cannot induce relocalization of the c-*ablPst* protein. The B64-Nh509 protein, which contains the less efficient kinase-activating region of *bcr*, was present at a higher concentration in the cytoplasm than in the nucleus, although nuclear staining was still observed in most cells (Fig. 4F). The localization of B64-Nh509 was predominantly diffuse, but in some cells increased staining of actin filaments was observed, especially along the thin edges of the cytoplasm (Fig. 4F). It appears that *bcr* amino acids 64 to 509 can also cause some increase in actin association. Addition of amino acids 39 to 63 to B64-Nh509, as in S39-Nh509, caused a slight increase in the staining of actin filaments relative to B64-Nh509 (data not shown). Staining of the actin meshwork around the cell edges and beneath the nucleus was more visible as a result of lower levels of diffuse staining in the cytoplasm. However, the localization of the S39-Nh509 protein was still more diffuse than that of B63, and low levels of this protein were detected in the nucleus. These results indicate that *bcr* amino acids 1 to 63, which strongly activate the c-*abl* kinase, also cause a large increase in its association with actin, whereas *bcr* amino acids 64 to 509, which weakly activate the kinase, cause a small increase in association with actin. The slight difference between B63 and Nh509 suggests that the effects of these two regions may be additive.

c-*abl* sequences are also required for microfilament association of *bcr/abl* proteins. The increased actin association of *bcr/abl* proteins could be due either to an actin-binding function of the *bcr* sequences or to enhancement of an intrinsic c-*abl* actin-binding function by the *bcr* sequences. To determine whether the normal *bcr* protein has the ability to associate with actin filaments, NIH 3T3 cells were transfected with a pLJbcr plasmid and cell lines which overproduced p160^{bcr} were isolated. When these cells were detergent extracted and the fractions were immunoblotted with antibodies for *bcr*, only 12% of the p160^{bcr} was recovered in the DIM fraction (Table 2). Double-label immunofluorescence with *bcr* antibodies and phalloidin showed that the *bcr* protein was localized primarily in the cytoplasm and did not colocalize of p160^{bcr} with actin filaments was observed (Fig. 5D to F). Thus, the increased actin association of *bcr/abl* proteins is probably not due to an actin-binding function of the *bcr* sequences.

If *bcr* enhances a c-*abl* actin-binding function, it should be possible to eliminate the association of *bcr/abl* proteins with actin filaments by making deletions in the c-*abl* sequence. A deletion was made in Nh509 which removes 80% of the unique, noncatalytic C-terminal domain of c-*abl* (Fig. 1B, *bcr*Nh509/c-*ablPst*-Nar). When the localization of this truncated protein was examined by immunofluorescence, it was found to distribute diffusely throughout the cytoplasm, and no colocalization with actin filaments was observed (Fig. 4C). This deletion specifically affected actin association, as the Nh509/Nar protein was still excluded from the nucleus and was still autophosphorylated (Fig. 4C; Table 1). This suggests that *bcr* may enhance an actin-binding function located within the C-terminal domain of c-*abl*. If this is the case, it could do so either indirectly by activating the c-*abl* autokinase, which would in turn enhance actin binding, or directly by altering the conformation of a c-*abl* actin-binding domain. To distinguish between these two mechanisms, the localization of the kinase-defective mutant, Nh509/His, was examined by immunofluorescence. The localization of the Nh509/His protein was found to be indistinguishable from that of Nh509 (data not shown). Therefore, the enhanced actin-association of *bcr/abl* proteins is not dependent on the kinase activity.

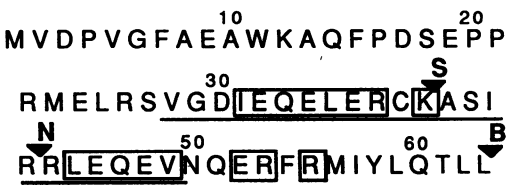

FIG. 6. Amino acid sequence of the N-terminal kinase-activating domain of *bcr* (amino acids 1 to 63). The putative amphipathic α-helix is underlined. The short imperfect repeats are boxed. Positions of deletions made in this region and the restriction enzymes used to create them are indicated in bold type above the sequence (see Fig. 1A and B for structures and phenotypes of these deletion mutants).

DISCUSSION

We have demonstrated that the *bcr* sequences of *bcr/abl* proteins are required for deregulation of the fused c-*abl* tyrosine kinase. The N-terminal 63 amino acids of *bcr* were found to be sufficient for this deregulation. A second region of *bcr* located between amino acids 64 and 509 was also capable of deregulating the fused c-*abl* kinase, but with much lower efficiency than the first 63 amino acids. The fusion proteins containing the N-terminal region of *bcr* were excluded from the nucleus and had an increased association with the actin cytoskeleton. The fusion protein containing amino acids 64 to 509 was partially excluded from the nucleus and showed a smaller increase in actin association. The increased actin association was apparently due to enhancement of an intrinsic microfilament-binding function of c-*abl* by the fused *bcr* sequences. Our results show that *bcr* sequences lead to kinase activation and increased actin association of *bcr/abl* proteins. However, these two properties are not interdependent, as a kinase-negative *bcr/abl* mutant was still associated with actin filaments and a *bcr/abl* mutant lacking c-*abl* sequences required for actin association still had deregulated kinase activity.

Structure of the N-terminal kinase-activating domain of *bcr*. The sequence of *bcr* amino acids 1 to 63 is shown in Fig. 6 (19). This domain is predicted to be α-helical with reverse turns at amino acids 18 to 21 and 69 to 72 (7, 18). Following this domain is a proline- and alanine-rich region between amino acids 80 and 150 with little predicted potential to form α-helices or β-sheets (7, 18, 19). This suggests that the N-terminal 70 amino acids of *bcr* may form an independent structural and functional domain. The region between amino acids 28 and 55 has two interesting features. First, there is a heptad repeat of hydrophobic amino acids from amino acids 28 to 49, with additional hydrophobic residues at the fourth position of two of the repeats (Fig. 6, underlined sequence). This region may be capable of forming a long, amphipathic α-helix. Such helices can mediate homo- or heterodimeric interactions between proteins. Second, the region contains two copies of a short, imperfect repeat with the consensus

XEQEX–ERXB, where X are hydrophobic residues and B is a basic residue (Fig. 6, boxed residues). Our deletion analysis suggests that this region containing the putative amphipathic helix and short repeats is necessary for the function of the N-terminal kinase-activating domain (Fig. 1B, N43 and S39-Nh509, and Fig. 6).

Mechanism for deregulation of the c-*abl* kinase by *bcr*. The behavior of the c-*abl* autokinase activity suggests that it is under tight negative regulation by *trans*-acting factors in mammalian cells. PTyr can never be detected on the c-*abl* protein in vivo, yet the autokinase invariably becomes activated whenever it is removed from the context of the mammalian cell or expressed to extremely high levels in COS cells (44a, 50). Regulation of autokinase activity requires the N-terminal noncatalytic domain of c-*abl*. This domain contains two regions of homology to the *src* family of cytoplasmic tyrosine protein kinases: SH3 and SH2 (42). The SH3 region appears to be necessary for inhibition of the c-*abl* autokinase in vivo (17, 25). Our results indicate that the effect of *bcr* on the c-*abl* autokinase activity is not equivalent to that of deletion of the SH3 domain. We consistently observed that the stoichiometry of tyrosine phosphorylation of *bcr/abl* proteins was 5- to 10-fold higher than that of the *gag*/v-*abl* and c-*abl*Hinc proteins which contain deletions of the SH3 box (Table 1). This suggests that *bcr* may act through another regulatory domain of c-*abl* besides SH3. Comparison of *bcr/abl* proteins with other activated *abl* proteins provides a clue to how *bcr* may interfere with the normal regulatory mechanism. Like *bcr/abl* proteins, the activated *abl* protein (fv-*abl*) encoded by Hardy-Zuckerman feline sarcoma virus has a short N-terminal deletion but retains the SH3 region (3). However, unlike *bcr/abl*, most of the C-terminal domain of c-*abl* is deleted in fv-*abl*. Shore et al. (45) have shown that an N-terminal deletion like that found in fv-*abl* partially activates c-*abl* and that an amino acid substitution at codon 832 in the C-terminal domain greatly enhances this activation.

Taken together, the data collected thus far suggests that an intramolecular interaction between the SH3 domain and the C-terminal domain may be necessary for inhibition of c-*abl* kinase activity. In murine v-*abl* this interaction would be disrupted by deletion of the SH3 domain, whereas in fv-*abl* it would be disrupted by deletion of the C-terminal domain. The evidence presented here suggests that *bcr* enhances a c-*abl* actin-binding function located in the C-terminal domain. It may be that an interaction of *bcr* sequences with either the SH3 or C-terminal domains of c-*abl* disrupts or alters an interaction between the two, resulting in a conformation change which activates the kinase as well as the actin-binding function.

Role of *bcr* and c-*abl* sequences in microfilament binding. Indirect immunofluorescence studies have shown that a small fraction of c-*abl* protein is associated with stress fibers upon overexpression in fibroblasts (38b, 48). This suggests that the c-*abl* protein has an intrinsic microfilament-binding activity. This is supported by sequence similarity between c-*abl* and some actin-binding proteins. Several actin-binding or membrane skeleton-associated proteins contain the SH3 motif, including nonerythroid α-spectrin, myosin 1B, the neutrophil oxidase factors p47 and p67, and the *Saccharomyces cerevisiae* ABP1 protein (12, 26, 31, 32, 44). The SH3 boxes of myosin 1B and ABP1 are adjacent to proline-rich sequences, and the ATP-insensitive actin-binding site of myosin 1B has been mapped to its proline-rich and SH3 regions (12, 36, 44). Interestingly, the noncatalytic C-terminal domain of c-*abl* is also extremely rich in proline. Moreover, we have shown that deletion of this proline-rich C-terminal domain eliminates the association of *bcr/abl* and c-*abl* proteins with actin filaments (Fig. 4C) (38a). Together, these similarities suggest that in addition to its role in tyrosine kinase regulation, the SH3 domain may regulate binding of these proline-rich domains to actin filaments. Our results suggest that the *bcr* sequences of *bcr/abl* proteins shift *abl* from an inactive conformation which does not bind to microfilaments and has low autokinase activity to an active conformation which binds microfilaments and has high autokinase activity. This raises the possibility that normal c-*abl* protein is targeted to microfilaments in response to some activating signal.

Role of actin association in normal c-*abl* function and in leukemogenesis. Although the function of the c-*abl* protein in mammalian cells is unknown, recent evidence suggests that the *Drosophila abl* homolog (D-*abl*) is involved in cell adhesion. A genetic interaction has been detected between D-*abl* and the gene for fascilin I, a neural cell adhesion molecule (15). This suggests that the D-*abl*, and perhaps the mammalian c-*abl*, protein may be part of a pathway regulating cell adhesion. However, in *Drosophila* cells the D-*abl* protein is expressed primarily in central nervous system axons during embryogenesis, whereas the c-*abl* protein is ubiquitously expressed in mammalian tissues and is localized in the nucleus as well as the cytoplasm. This suggests that c-*abl* function may have diverged considerably between insects and mammals. Nevertheless, the ability of c-*abl* protein to associate with the actin cytoskeleton may allow it to interact directly with cell surface molecules involved in cell-cell or cell-substratum interactions.

Localization of *bcr/abl* fusion proteins in the actin cytoskeleton of CML and Ph′-positive ALL cells may be an important factor in these leukemias. Experiments by Eaves et al. (13, 14) suggest that the proliferation of normal hematopoietic progenitor cells is controlled by a negative regulatory signal produced by nonhematopoietic, mesenchymal bone marrow cells. The mechanism of growth inhibition may involve direct cell contact. Ph′-positive hematopoietic progenitor cells from patients with CML, however, continue to proliferate even in the presence of this growth-inhibitory signal (13, 14). We have found that the majority of PTyr-containing proteins in the CML cell line K562 are preferentially associated with the detergent-insoluble cytoskeletal matrix, so components of the cytoskeletal framework may be the principal substrates of the *bcr/abl* kinase (38b). It is possible that the *bcr/abl* kinase phosphorylates substrates in the cytoskeleton that are involved in the interaction of hematopoietic stem cells with mesenchymal bone marrow cells. Phosphorylation of these substrates might block transduction of the growth-inhibitory signal, allowing unregulated growth of the Ph′-positive stem cells.

ACKNOWLEDGMENTS

We are grateful to John Groffen for his gift of the *bcr* cDNA clone, to Ralph B. Arlinghaus for his gift of anti-*bcr* peptide antiserum, and to Susan K. Sullivan for the preparation of t/bcr antiserum. We also thank Kiyoteru Tokuyasu for help with immunofluorescence and the use of his fluorescence microscope and Tony Hunter for comments on the manuscript.

This work was supported by National Institutes of Health grant CA43054.

REFERENCES

1. **Arlinghaus, R. B.** Personal communication.

1a. **Ben-Neriah, Y., G. Q. Daley, A. M. Mes-Masson, O. N. Witte,**

and D. Baltimore. 1986. The chronic myelogenous leukemia-specific P210 protein is the product of the bcr/abl hybrid gene. Science **233**:212–214.

2. **Ben-Ze'ev, A., A. Duerr, F. Solomon, and S. Penman.** 1979. The outer boundary of the cytoskeleton: a lamina derived from plasma membrane proteins. Cell **17**:859–865.
3. **Bergold, P. J., J. A. Blumenthal, E. D'Andrea, H. W. Snyder, L. Lederman, A. Silverstone, H. Nguyen, and P. Besmer.** 1987. Nucleic acid sequence and oncogenic properties of the HZ2 feline sarcoma virus v-*abl* insert. J. Virol. **61**:1193–1202.
4. **Boss, M. A., G. Dreyfuss, and D. Baltimore.** 1981. Localization of the Abelson murine leukemia virus protein in a detergent-insoluble matrix: architecture of the protein. J. Virol. **40**:472–481.
5. **Cervera, M., G. Dreyfuss, and S. Penman.** 1981. Messenger RNA is translated when associated with the cytoskeletal framework in normal and VSV-infected HeLa cells. Cell **23**:113–120.
6. **Chan, L. C., K. K. Karhi, S. I. Rayter, N. Heistercamp, S. Eridani, R. Powles, S. D. Lawler, J. Groffen, J. G. Foulkes, M. F. Greaves, and L. M. Wiedemann.** 1987. A novel abl protein expressed in Philadelphia chromosome positive acute lymphoblastic leukemia. Nature (London) **325**:635–637.
7. **Chou, P. Y., and G. D. Fasman.** 1978. Prediction of the secondary structure of proteins from their amino acid sequence. Adv. Enzymol. **47**:45–147.
8. **Clark, S. S., J. McLaughlin, M. Timmons, A. M. Pendergast, Y. Ben-Neriah, L. W. Dow, W. Crist, G. Rovera, S. D. Smith, and O. N. Witte.** 1988. Expression of a distinctive bcr/abl oncogene in Ph^1-positive acute lymphocytic leukemia (ALL). Science **239**:775–777.
9. **Daley, G. Q., and D. Baltimore.** 1988. Transformation of an interleukin 3-dependent hematopoietic cell line by the chronic myelogenous leukemia-specific $p210^{bcr/abl}$ protein. Proc. Natl. Acad. Sci. USA **85**:9312–9316.
10. **Daley, G. Q., R. A. Van Etten, and D. Baltimore.** 1990. Induction of chronic myelogenous leukemia in mice by the $p210^{bcr/abl}$ gene of the Philadelphia chromosome. Science **247**:824–830.
11. **de Klein, A., A. D. van Kessel, G. Grosveld, C. R. Bartram, A. Hagemeijer, D. Bootsma, N. K. Spurr, N. Heistercamp, J. Groffen, and J. R. Stephenson.** 1982. A cellular oncogene is translocated to the Philadelphia chromosome in chronic myelocytic leukaemia. Nature (London) **300**:765–767.
12. **Drubin, D. G., J. Mulholland, Z. Zhu, and D. Botstein.** 1990. Homology of a yeast actin-binding protein to signal transduction proteins and myosin-I. Nature (London) **343**:288–290.
13. **Eaves, A. C., J. D. Cashman, L. A. Gaboury, D. K. Kalousek, and C. J. Eaves.** 1986. Unregulated proliferation of primitive chronic myeloid leukemia progenitors in the presence of normal marrow adherent cells. Proc. Natl. Acad. Sci. USA **83**:5306–5310.
14. **Eaves, A. C., and C. J. Eaves.** 1988. Maintenance and proliferation control of primitive hemopoietic progenitors in long-term cultures of human marrow cells. Blood Cells **14**:355–368.
15. **Elkins, T., K. Zinn, L. McAllister, F. M. Hoffman, and C. S. Goodman.** 1990. Genetic analysis of a Drosophila neural cell adhesion molecule: interaction of fascilin I and Abelson tyrosine kinase mutations. Cell **60**:565–575.
16. **Fainstein, E., M. Einat, E. Gokkel, C. Marcelle, C. M. Croce, R. P. Gale, and E. Canaani.** 1989. Nucleotide sequence analysis of human abl and bcr-abl cDNAs. Oncogene **4**:1477–1482.
17. **Franz, W. M., P. Berger, and J. Y. J. Wang.** 1989. Deletion of an N-terminal regulatory domain of the c-abl tyrosine kinase activates its oncogenic potential. EMBO J. **8**:137–147.
18. **Garnier, J., D. J. Osguthorpe, and B. Robson.** 1978. Analysis of the accuracy and implications of simple methods for predicting the secondary structure of globular proteins. J. Mol. Biol. **120**:97–120.
19. **Hariharan, I. K., and J. M. Adams.** 1987. cDNA sequence for human bcr, the gene that translocates to the abl oncogene in chronic myeloid leukaemia. EMBO J. **6**:115–119.
20. **Heistercamp, N., G. Jenster, J. ten Hoeve, D. Zovich, P. K. Pattengale, and J. Groffen.** 1990. Acute leukemia in bcr/abl transgenic mice. Nature (London) **344**:251–253.
21. **Heisterkamp, N., E. Knoppel, and J. Groffen.** 1988. The first bcr gene intron contains breakpoints in Philadelphia chromosome positive leukemia. Nucleic Acids Res. **16**:10069–10081.
22. **Heisterkamp, N., K. Stam, and J. Groffen.** 1985. Structural organization of the bcr gene and its role in the Ph' translocation. Nature (London) **315**:758–761.
23. **Heisterkamp, N., J. R. Stephenson, J. Groffen, P. F. Hansen, A. de Klein, C. R. Bartram, and G. Grosveld.** 1983. Localization of the c-abl oncogene adjacent to a translocation break point in chronic myelocytic leukaemia. Nature (London) **306**:239–242.
24. **Hermans, A., N. Heisterkamp, M. von Lindern, S. van Baal, D. Meijer, D. van der Plas, L. M. Wiedemann, J. Groffen, D. Bootsma, and G. Grosveld.** 1987. Unique fusion of bcr and c-abl genes in Philadelphia chromosome positive acute lymphoblastic leukemia. Cell **51**:33–40.
25. **Jackson, P., and D. Baltimore.** 1989. N-terminal mutations activate the leukemogenic potential of the myristoylated form of c-abl. EMBO J. **8**:449–456.
26. **Jung, G., E. D. Korn, and J. A. Hammer.** 1987. The heavy chain of Acanthamoeba myosin 1B is a fusion of myosin-like and non-myosin-like sequences. Proc. Natl. Acad. Sci. USA **84**:6720–6724.
27. **Konopka, J. B., S. M. Watanabe, and O. N. Witte.** 1984. An alteration of the human c-abl protein in K562 leukemia cells unmasks associated tyrosine kinase activity. Cell **37**:1035–1042.
28. **Konopka, J. B., and O. N. Witte.** 1985. Detection of c-*abl* tyrosine kinase activity in vitro permits direct comparison of normal and altered *abl* gene products. Mol. Cell. Biol. **5**:3116–3123.
29. **Korman, A. L., J. L. Frantz, J. L. Stominger, and R. C. Mulligan.** 1987. Expression of human class II major histocompatibility complex antigens using retrovirus vectors. Proc. Natl. Acad. Sci. USA **84**:2150–2154.
30. **Kurzrock, R., M. Shtalrid, P. Romero, W. S. Kloetzer, M. Talpas, J. M. Trujillo, M. Blick, M. Beran, and J. U. Gutterman.** 1987. A novel c-abl protein product in Philadelphia-positive acute lymphoblastic leukaemia. Nature (London) **325**:631–637.
31. **Lehto, V. P., V. M. Wasenious, P. Salven, and M. Saraste.** 1988. Transforming and membrane proteins. Nature (London) **334**:388.
32. **Leto, T. L., K. L. Lomax, B. D. Volpp, H. Nunoi, J. M. G. Sechler, W. M. Nauseef, R. A. Clark, J. I. Gallin, and H. L. Malech.** 1990. Cloning of a 67-kD neutrophil oxidase factor with similarity to a noncatalytic region of $p60^{c\text{-}src}$. Science **248**:727–730.
33. **Lozzio, C. B., and B. B. Lozzio.** 1975. Human chronic myelogenous leukemia cell line with positive Philadelphia chromosome. Blood **45**:321–334.
34. **Lugo, T. G., A. M. Pendergast, and O. N. Witte.** 1990. Tyrosine kinase activity and transformation potency of *bcr-abl* gene products. Science **247**:1079–1082.
35. **Lugo, T. G., and O. N. Witte.** 1989. The BCR/ABL oncogene transforms Rat-1 cells and cooperates with v-*myc*. Mol. Cell. Biol. **9**:1263–1270.
36. **Lynch, T. J., J. P. Albanesi, E. D. Korn, E. A. Robinson, B. Bowers, and H. Fujisaki.** 1986. ATPase activities and actin-binding properties of subfragments of Acanthamoeba myosin IA. J. Biol. Chem. **261**:17156–17162.
37. **McLaughlin, J., E. Chianese, and O. N. Witte.** 1987. In vitro transformation of immature hematopoietic cells by the P210 bcr/abl oncogene product of the Philadelphia chromosome. Proc. Natl. Acad. Sci. USA **84**:6558–6562.
38. **McLaughlin, J., E. Chianese, and O. N. Witte.** 1989. Alternative forms of the *BCR-ABL* oncogene have quantitively different potencies for stimulation of immature lymphoid cells. Mol. Cell. Biol. **9**:1866–1874.

38a. **McWhirter, J. R., S. M. Seaton, and J. Y. J. Wang.** Unpublished data.

38b. **McWhirter, J. R., and J. Y. J. Wang.** Unpublished data.

39. **Mes-Masson, A. M., J. McLaughlin, G. Q. Daley, M. Paskind, and O. N. Witte.** 1986. Overlapping cDNA clones define the complete coding region for the $P210^{c\text{-}abl}$ gene product associated with chronic myelogenous leukemia cells containing the Phila-

delphia chromosome. Proc. Natl. Acad. Sci. USA **83**:9768–9772.

40. **Naldini, L., A. Stacchini, D. M. Cirillo, M. Aglietta, F. Gavosto, and P. M. Comoglio.** 1986. Phosphotyrosine antibodies identify the $p210^{c\text{-}abl}$ tyrosine kinase and proteins phosphorylated on tyrosine in human chronic myelogenous leukemia cells. Mol. Cell. Biol. **6**:1803–1811.
41. **Oppi, C., S. K. Shore, and E. P. Reddy.** 1987. Nucleotide sequence of testis-derived c-abl cDNAs: implications for testis-specific transcription and abl oncogene activation. Proc. Natl. Acad. Sci. USA **84**:8200–8204.
42. **Pawson, T.** 1988. Noncatalytic domains of cytoplasmic protein-tyrosine kinases: regulatory elements in signal transduction. Oncogene **3**:491–495.
43. **Richardson, J. M., A. O. Morla, and J. Y. J. Wang.** 1987. Reduction in protein tyrosine phosphorylation during differentiation of human leukemia cell line K562. Cancer Res. **47**:4066–4070.
44. **Rodaway, A. R. F., M. J. E. Sternberg, and D. L. Bentley.** 1989. Similarity in membrane proteins. Nature (London) **342**:624.

44a. **Seaton, S. M., and J. Y. J. Wang.** Unpublished data.

45. **Shore, S. K., S. L. Bogart, and E. P. Reddy.** 1990. Activation of murine c-abl protooncogene: effect of a point mutation on oncogenic activation. Proc. Natl. Acad. Sci. USA **87**:6502–6506.
46. **Shtivelman, E., B. Lifshitz, R. P. Gale, and E. Canaani.** 1985. Fused transcript of abl and bcr genes in chronic myelogenous leukemia. Nature (London) **315**:550–554.
47. **Shtivelman, E., B. Lifshitz, R. P. Gale, B. A. Roe, and E. Canaani.** 1986. Alternative splicing of RNAs transcribed from the human abl gene and from the bcr-abl fused gene. Cell **47**:277–284.

47a. **Trepanier, M., and J. Y. J. Wang.** Unpublished data.

48. **Van Etten, R. A., P. Jackson, and D. Baltimore.** 1989. The mouse type IV c-abl gene product is a nuclear protein, and activation of transforming ability is associated with cytoplasmic localization. Cell **58**:669–678.
49. **Wang, J. Y. J.** 1985. Isolation of antibodies for phosphotyrosine by immunization with a v-*abl* oncogene-encoded protein. Mol. Cell. Biol. **5**:3640–3643.
50. **Wang, J. Y. J.** 1988. Negative regulation of c-abl tyrosine kinase by its variable N-terminal amino acids. Oncogene Res. **3**:293–298.
51. **Wang, J. Y. J., and D. Baltimore.** 1983. Cellular RNA homologous to the Abelson murine leukemia virus transforming gene: expression and relationship to the viral sequence. Mol. Cell. Biol. **3**:773–779.
52. **Wang, J. Y. J., and D. Baltimore.** 1985. Localization of tyrosine kinase-coding region in v-abl oncogene by the expression of v-abl-encoded proteins in bacteria. J. Biol. Chem. **260**:64–71.
53. **Wang, J. Y. J., F. Ledley, S. Goff, R. Lee, Y. Groner, and D. Baltimore.** 1984. The mouse c-abl locus: molecular cloning and characterization. Cell **36**:349–356.
54. **Young, J. C., and O. N. Witte.** 1988. Selective transformation of primitive lymphoid cells by the *BCR/ABL* oncogene expressed in long-term lymphoid or myeloid cultures. Mol. Cell. Biol. **8**:4079–4087.